Design of Nonlinear Decoupling Controller for Double-electromagnet Suspension System[1)]

LIU De-Sheng LI Jie ZHANG Kun

(*College of Mechatronics Engineering and Automation, National University of Defense Technology, Changsha* 410073)

(E-mail: deshengnudt@163.com)

Abstract Aiming at the coupling characteristic between the two groups of electromagnets embedded in the module of the maglev train, a nonlinear decoupling controller is designed. The module is modeled as a double-electromagnet system, and based on some reasonable assumptions its nonlinear mathematical model, a MIMO coupling system, is derived. To realize the linearization and decoupling from the input to the output, the model is linearized exactly by means of feedback linearization, and an equivalent linear decoupling model is obtained. Based on the linear model, a nonlinear suspension controller is designed using state feedback. Simulations and experiments show that the controller can effectually solve the coupling problem in double-electromagnet suspension system.

Key words Double-electromagnet, nonlinear, decoupling, suspension controller, feedback linearization

1 Introduction

Electromagnetic suspension (EMS) type low speed maglev train usually adopts modular magnetic bogie structure. The magnetic bogie is composed of two modules which are connected with two sets of roll-beams and brace the chassis through air springs. Reference [1] proved that reasonable structure design can realize mechanical decoupling between the two modules by roll-beams. Therefore, the suspension control of the maglev train can be simplified as a control problem of the module suspension system. The module mainly includes a linear motor stator, four suspension electromagnets and a box girder. The four electromagnets are divided into two groups along the forward direction of the train. Generally each group of electromagnets is regarded as a single electromagnet, which is independent of the control degrees of freedom; thus the module suspension system usually is decomposed into two independent single electromagnet suspension systems to design controllers, respectively.

In fact, the two groups of electromagnets embedded in a module are connected with a rigid body, and their motion states are coupling. At present the general control method controls the two groups of electromagnets separately using two independent controllers, and each acts according to the respective controlled object; the coupling between the two groups of electromagnets is regarded as disturbance and suppressed by enhancing the robustness of the controller[2~7]. However, this method can not actively overcome the coupling question, and the control performance is not desirable when the system is adjusting due to the disturbance.

In this paper, the module is modeled as a double-electromagnet (DEM) suspension system, and the method to solve the coupling problem of module suspension system is studied based on a DEM prototype.

2 System modeling

2.1 Construction of the system

The construction of the DEM suspension system is shown in Fig. 1. It contains two identical electromagnets that are connected with a rigid bracket. Electromagnet 1 and electromagnet 2 provide suspension forces for point A and point B, respectively. The suspension object can be regarded as a rigid body with two electromagnets. The sensors are used to measure suspension states and the poises are used to exert load forces.

The DEM suspension system can be simplified as shown in Fig. 2. The parameters are defined as follows: m is the mass of the suspension object, I is the rotation inertia to the geometry center O, F_1 and F_2 are electromagnetic forces, N_1 and N_2 are loads that are exerted to each end of the bracket

1) Supported by National Natural Science Foundation of P. R. China (60404003), the Natural Science Foundation of Hunan Province (03JJY3108), and Fok Ying-Tong Education Foundation (94028)

Received November 3, 2004; in revised form November 22, 2005

respectively, d is the distance from the rail to O, δ_1 and δ_2 are the distances from the rail to the action points of F_1 and F_2, d_1 and d_2 are the gap values from sensors, l is the distance from O to the action points of electromagnetic forces, and L is the distances from O to the action point of the load forces.

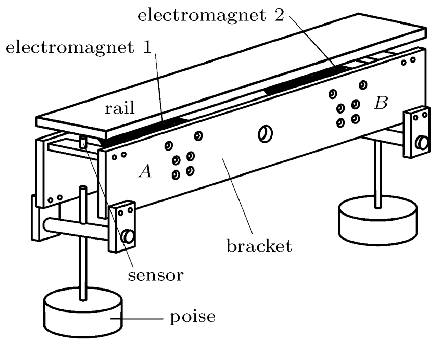

Fig. 1 Construction of the DEM suspension system

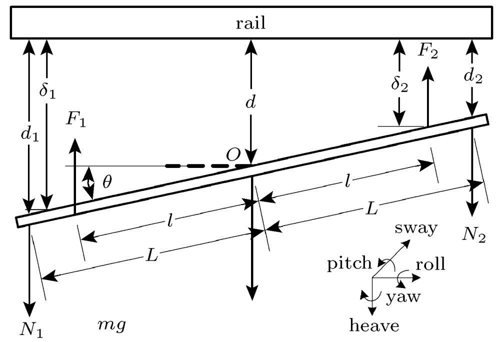

Fig. 2 Simplified model of the DEM suspension system

In the range of the model precision permission, some reasonable assumptions are introduced as follows.

1) The stiffness of the rail is infinite and only the relative motion of the DEM relative to the rail is considered.

2) The leakage flux and the magnetic field edge effect are neglected, and the magnetic resistances of the ferrite core and the rail are neglected, *i.e.*, the magnetic potential falls on the air gap evenly.

3) The distribution of the mass of the bracket is even, and the masses of the two magnets are equal, so the action point of gravity is superposed on the geometry center O.

4) The length of the electromagnet relative to the bracket and the obliquity θ are very small, and the action point of the electromagnetic force is considered stationary.

5) The action line of the load forces is superposed with the direction of the gap measured.

Under these assumptions, the mathematical model of the DEM suspension system is derived in the followings.

2.2 Mathematical model

The DEM suspension system is a complex mechanical and electrical system, which contains the mechanical dynamics of DEM, the relation between the current and the electromagnetic force, and the relation between the voltage and the current.

1) Mechanical dynamics equation

The DEM system has five degrees of motion freedom, *i.e.*, heave, sway, pitch, roll and yaw[8], as shown in Fig. 2. For the suspension controller only the motions of heave and pitch should be considered. The heave motion is the translation at the centroid O and the pitch motion is the rotation round the centroidal principal axis. The positive directions of the translation and the rotation are downward and anticlockwise, respectively. According to the translation principle of force and the Newton second law of motion, the mechanical dynamics equations are given by

$$\begin{cases} m\ddot{d} = -F_1 - F_2 + N_1 + N_2 + mg \\ I\ddot{\theta} = N_1 L - N_2 L - F_1 l + F_2 l \end{cases} \tag{1}$$

From Fig. 2, we have

$$d = (d_1 + d_2)/2, \quad \theta \approx (d_1 - d_2)/2L \tag{2}$$

Substitution of (2) into (1) gives

$$\begin{cases} \ddot{d}_1 = -A_K \times F_1 - B_K \times F_2 + C_K \times N_1 + D_K \times N_2 + g \\ \ddot{d}_2 = -B_K \times F_1 - A_K \times F_2 + D_K \times N_1 + C_K \times N_2 + g \end{cases} \tag{3}$$

where

$$A_K = \frac{1}{m} + \frac{Ll}{I}, \quad B_K = \frac{1}{m} - \frac{Ll}{I}, \quad C_K = \frac{1}{m} + \frac{L^2}{I}, \quad D_K = \frac{1}{m} - \frac{L^2}{I} \tag{4}$$

2) Magnetic force equation

The magnetic force between electromagnet and rail can be represented as $F = Ki^2/\delta^2$, where K is a characteristic feature constant, δ is the distance between electromagnet and rail, and i is the current flow in the coil. From Fig. 2, we have

$$\begin{cases} \delta_1 = d + \theta \times l = Pd_1 + Qd_2 \\ \delta_2 = d - \theta \times l = Qd_1 + Pd_2 \end{cases} \tag{5}$$

where $P = (L+l)/(2L)$, $Q = (L-l)/(2L)$. So the electromagnetic forces in Fig. 2 can be expressed by

$$\begin{cases} F_1 = K\dfrac{\dot{i}_1^2}{\delta_1^2} = K\dfrac{i_1^2}{(Pd_1 + Qd_2)^2} \\ F_2 = K\dfrac{\dot{i}_2^2}{\delta_2^2} = K\dfrac{i_2^2}{(Qd_1 + Pd_2)^2} \end{cases} \tag{6}$$

3) Electrical dynamics equation

The electrical dynamics of the electromagnetic suspension system can be treated as an inductance-resistance circuit and formulated as follows

$$u(t) = Ri + \frac{2K\dot{i}}{\delta} - \frac{2Ki\dot{\delta}}{\delta^2} \tag{7}$$

where $u(t)$ is the control voltage of the electromagnet, R is the total resistance of the electrical circuit. Substituting (5) into (7), we obtain the electrical dynamics equations for the two electromagnets as follows

$$\begin{cases} u_1(t) = Ri_1 + \dfrac{2K\dot{i}_1}{Pd_1 + Qd_2} - \dfrac{2Ki_1(P\dot{d}_1 + Q\dot{d}_2)}{(Pd_1 + Qd_2)^2} \\ u_2(t) = Ri_2 + \dfrac{2K\dot{i}_2}{Qd_1 + Pd_2} - \dfrac{2Ki_2(Q\dot{d}_1 + P\dot{d}_2)^2}{(Qd_1 + Pd_2)} \end{cases} \tag{8}$$

where $u_1(t)$ and $u_2(t)$ are the control voltages of the two electromagnets, respectively.

On all accounts above, the mathematical model of DEM suspension system in Fig. 1 can be described by (3), (6), and (8), that is,

$$\begin{cases} \ddot{d}_1 = -A_K \times F_1 - B_K \times F_2 + C_K \times N_1 + D_K \times N_2 + g \\ \ddot{d}_2 = -B_K \times F_1 - A_K \times F_2 + D_K \times N_1 + C_K \times N_2 + g \\ F_1 = K\dfrac{i_1^2}{\delta_1^2} = K\dfrac{i_1^2}{(Pd_1 + Qd_2)^2} \\ F_2 = K\dfrac{i_2^2}{\delta_2^2} = K\dfrac{i_2^2}{(Qd_1 + Pd_2)^2} \\ u_1(t) = Ri_1 + \dfrac{2K}{Pd_1 + Qd_2}\dot{i}_1 - \dfrac{2Ki_1}{(Pd_1 + Qd_2)^2}(P\dot{d}_1 + Q\dot{d}_2) \\ u_2(t) = Ri_2 + \dfrac{2K}{Qd_1 + Pd_2}\dot{i}_2 - \dfrac{2Ki_2}{(Qd_1 + Pd_2)^2}(Q\dot{d}_1 + P\dot{d}_2) \end{cases} \tag{9}$$

Considering the current flow in the coil can not track the given input value rapidly due to the inductance of the electromagnet, the idea of cascade control is introduced to design of the suspension controller[8], and the system is divided into two serial-connected decoupling subsystems: the current loop subsystem and the position loop subsystem. The current loop is designed as a proportional tache by current negative feedback. This scheme has been proved feasible in practice. Consequently, we just consider the design of controller for the position loop.

2.3 State-space equation

Assuming the current loop is rapid enough, and defining the state variable vector as $\boldsymbol{x} = [x_1, x_2, x_3, x_4]^{\mathrm{T}} = [d_1, \dot{d}_1, d_2, \dot{d}_2]^{\mathrm{T}}$, we have the following nonlinear state-space model

$$\begin{cases} \dot{\boldsymbol{x}} = \boldsymbol{f}(\boldsymbol{x}) + \mathbb{G}(\boldsymbol{x})\boldsymbol{u} \\ \boldsymbol{y} = \boldsymbol{h}(\boldsymbol{x}) \end{cases} \tag{10}$$

where

$$\boldsymbol{f}(\boldsymbol{x}) = \begin{bmatrix} x_2 \\ C_K N_1 + D_K N_2 + g \\ x_4 \\ D_K N_1 + C_K N_2 + g \end{bmatrix}, \ \boldsymbol{h}(\boldsymbol{x}) = \begin{bmatrix} h_1(\boldsymbol{x}) \\ h_2(\boldsymbol{x}) \end{bmatrix} = \begin{bmatrix} x_1 \\ x_3 \end{bmatrix}$$

$$\mathbb{G}(\boldsymbol{x}) = \begin{bmatrix} \boldsymbol{g}_1(\boldsymbol{x}) \\ \boldsymbol{g}_2(\boldsymbol{x}) \end{bmatrix}^{\mathrm{T}} = \begin{bmatrix} 0 & 0 \\ -\dfrac{A_K K}{(Px_1+Qx_3)^2} & -\dfrac{B_K K}{(Qx_1+Px_3)^2} \\ 0 & 0 \\ -\dfrac{B_K K}{(Px_1+Qx_3)^2} & -\dfrac{A_K K}{(Qx_1+Px_3)^2} \end{bmatrix}, \ \boldsymbol{u} = \begin{bmatrix} u_1 \\ u_2 \end{bmatrix} = \begin{bmatrix} i_1^2 \\ i_2^2 \end{bmatrix}$$

Obviously, the model (10) is a coupling system. For this kind of system, feedback linearization is usually used to realize the linearization and decoupling from its input to its output, thereby the design of controller can be simplified.

3 Feedback linearization

For a MIMO affine system[9]

$$\begin{cases} \dot{\boldsymbol{x}} = \boldsymbol{f}(\boldsymbol{x}) + \sum\limits_{i=1}^{m} \boldsymbol{g}_i(\boldsymbol{x}) u_i \\ \boldsymbol{y} = \boldsymbol{h}(\boldsymbol{x}) \end{cases} \tag{11}$$

given $\boldsymbol{x}_0 \in X$, there exist a feedback control $\boldsymbol{u} = \mathbb{E}^{-1}(\boldsymbol{x})[-\boldsymbol{b}(\boldsymbol{x}) + v]$ and a homeomorphous map $\boldsymbol{z} = \Phi(\boldsymbol{x})$ in a neighborhood V of $\boldsymbol{x}_0$, such that system (11) can be transformed into a linear decoupling system in new coordinates of $\boldsymbol{z}$ under the control of $\boldsymbol{u}$

$$\begin{cases} \dot{\boldsymbol{z}} = \mathbb{A}\boldsymbol{z} + \mathbb{B}\boldsymbol{v} \\ \boldsymbol{y} = \mathbb{C}\boldsymbol{z} \end{cases} \tag{12}$$

For the DEM suspension system (10), we validate the linearizable conditions firstly. Since

$$L_{g_1} L_f^0 h_1(\boldsymbol{x}) = 0, \ L_{g_2} L_f^0 h_1(\boldsymbol{x}) = 0, \ L_{g_1} L_f^0 h_2(\boldsymbol{x}) = 0, \ L_{g_2} L_f^0 h_2(\boldsymbol{x}) = 0$$

$$L_{g_1} L_f h_1(\boldsymbol{x}) = -\frac{A_K K}{(Px_1+Qx_3)^2} \neq 0, \ L_{g_2} L_f h_1(\boldsymbol{x}) = -\frac{B_K K}{(Qx_1+Px_3)^2} \neq 0$$

$$L_{g_1} L_f h_2(\boldsymbol{x}) = -\frac{B_K K}{(Px_1+Qx_3)^2} \neq 0, \ L_{g_2} L_f h_2(\boldsymbol{x}) = -\frac{A_K K}{(Qx_1+Px_3)^2} \neq 0$$

and there exists a matrix

$$\mathbb{E}(\boldsymbol{x}) = \begin{bmatrix} -\dfrac{A_K K}{(Px_1+Qx_3)^2} & -\dfrac{B_K K}{(Qx_1+Px_3)^2} \\ -\dfrac{B_K K}{(Px_1+Qx_3)^2} & -\dfrac{A_K K}{(Qx_1+Px_3)^2} \end{bmatrix}$$

such that $\det\mathbb{E}(\boldsymbol{x}) \neq 0$, *i.e.*, $\mathbb{E}(\boldsymbol{x})$ is not singular, the relative degree of the system is $(r_1, r_2) = (2, 2)$ and $r = r_1 + r_2 = 4$. Therefore, system (10) is linearizable.

Choosing feedback control law as

$$\boldsymbol{u} = \mathbb{E}^{-1}(\boldsymbol{x})[-\boldsymbol{b}(\boldsymbol{x}) + \boldsymbol{v}] \tag{13}$$

where

$$\mathbb{E}^{-1}(\boldsymbol{x}) = \frac{1}{K(A_K^2 - B_K^2)} \begin{bmatrix} -(Px_1+Qx_3)^2 A_K & (Px_1+Qx_3)^2 B_K \\ (Qx_1+Px_3)^2 B_K & -(Qx_1+Px_3)^2 A_K \end{bmatrix}$$

$$\boldsymbol{b}(\boldsymbol{x}) = [L_f^{r_1} h_1(\boldsymbol{x}) \quad L_f^{r_2} h_2(\boldsymbol{x})]^{\mathrm{T}} = [C_K N_1 + D_K N_2 + g \quad D_K N_1 + C_K N_2 + g]^{\mathrm{T}}$$

Substitution of (4) into (13) gives

$$\boldsymbol{u} = \begin{bmatrix} u_1 \\ u_2 \end{bmatrix} = \begin{bmatrix} (Px_1 + Qx_3)^2(K_{n\_m}N_1 + K_{n\_s}N_2 + K_g g - K_{v\_m}v_1 + K_{v\_s}v_2) \\ (Qx_1 + Px_3)^2(K_{n\_m}N_2 + K_{n\_s}N_1 + K_g g - K_{v\_m}v_2 + K_{v\_s}v_1) \end{bmatrix} \tag{14}$$

where

$$K_{n\_m} = \frac{l+L}{2KL},\ K_{n\_s} = \frac{l-L}{2Kl},\ K_g = \frac{m}{2K},\ K_{v\_m} = \frac{I+mLl}{4KLl},\ k_{v\_s} = \frac{I-mLl}{4KLl}$$

The homeomorphous map $\boldsymbol{z} = \Phi(\boldsymbol{x})$

$$\boldsymbol{z} = [h_1(\boldsymbol{x}) \quad L_f h_1(\boldsymbol{x}) \quad h_2(\boldsymbol{x}) \quad L_f h_2(\boldsymbol{x})]^{\mathrm{T}} = [x_1 \quad x_2 \quad x_3 \quad x_4]^{\mathrm{T}} \tag{15}$$

Accordingly, in these new coordinates the state-space equations of system (10) become

$$\begin{cases} \dot{\boldsymbol{z}} = \mathbb{A}\boldsymbol{z} + \mathbb{B}\boldsymbol{v} \\ \boldsymbol{y} = \mathbb{C}\boldsymbol{z} \end{cases} \tag{16}$$

where

$$\mathbb{A} = \begin{bmatrix} 0 & 1 & 0 & 0 \\ 0 & 0 & 0 & 0 \\ 0 & 0 & 0 & 1 \\ 0 & 0 & 0 & 0 \end{bmatrix},\ \mathbb{B} = \begin{bmatrix} 0 & 0 \\ 1 & 0 \\ 0 & 0 \\ 0 & 1 \end{bmatrix},\ \mathbb{C} = \begin{bmatrix} 1 & 0 & 0 & 0 \\ 0 & 0 & 1 & 0 \end{bmatrix}$$

The transfer function matrix of the system is given by

$$\mathbb{G}(s) = \begin{bmatrix} \frac{1}{s^2} & 0 \\ 0 & \frac{1}{s^2} \end{bmatrix} \tag{17}$$

The original system becomes a typical integral type decoupling system after feedback linearization. The state variables of the two subsystems are gap, and velocity and current; there is no coupling between the two groups of state variables, namely we realize the electrical decoupling for the original system. We can accomplish the design of the controller for the DEM suspension system by designing the control law $\boldsymbol{v}$ for decoupling system (16).

4 Nonlinear controller design and analysis

4.1 Controller design

The controllability matrix of system (16) is

$$\mathbb{M} = \begin{bmatrix} 0 & 0 & 1 & 0 & 0 & 0 & 0 & 0 \\ 1 & 0 & 0 & 0 & 0 & 0 & 0 & 0 \\ 0 & 0 & 0 & 1 & 0 & 0 & 0 & 0 \\ 0 & 1 & 0 & 0 & 0 & 0 & 0 & 0 \end{bmatrix}$$

Since rank$(\mathbb{M}) = 4$, system (16) is completely controllable. So that we can design the controller by means of pole placement. As system (16) is a decoupling system, controllers v_1 and v_2 can be designed, respectively. Without loss of generality, we take v_1 as an example to explain the design of controller.

By means of state feedback and input transform, the control law is given by

$$v_1 = R_1 v_{c1} - \boldsymbol{k}_1 \boldsymbol{y}_1 \tag{18}$$

where $\boldsymbol{y}_1 = [z_1 \quad z_2]^{\mathrm{T}}$, $\boldsymbol{k}_1 = [k_{11} \quad k_{12}]$ is the gain vector of state feedback, R_1 is the coefficient of the input transform, and v_{c1} is the given gap value. According to the desired dynamic response of the close loop system, we choose the desired poles as $\lambda_{1,2} = -35.35 \pm j35.35$. By means of pole placement, we obtain the gains of feedback $k_{11} = 2500$, $k_{12} = 70.7$. Then the close loop transfer function is given by

$$G_L(s) = \frac{R_1}{s^2 + 70.7s + 2500} \tag{19}$$

Generally, we desire the steady error to satisfy $e_p = 0$, *i.e.*, the steady gain is 1

$$\lim_{s\to 0} G_L(s) = 1 \Rightarrow \lim_{s\to 0} \frac{R_1}{s^2 + 70.7s + 2500} = 1 \Rightarrow R_1 = 2500$$

Therefore

$$v_1 = R_1 v_{c1} - \boldsymbol{k}_1 \boldsymbol{y}_1 = 2500 v_{c1} - 2500 z_1 - 70.7 z_2 = 2500(v_{c1} - d_1) - 70.7 \dot{d}_1 \tag{20}$$

Similarly, v_2 is given by

$$v_2 = 2500(v_{c2} - d_2) - 70.7 \dot{d}_2 \tag{21}$$

From equation (14), we can obtain the control laws for currents as follows

$$\boldsymbol{i} = \begin{bmatrix} i_1 \\ i_2 \end{bmatrix} = \begin{bmatrix} (Px_1 + Qx_3)\sqrt{(K_{n\_m}N_1 + K_{n\_s}N_2 + K_g g - K_{v\_m}v_1 + K_{v\_s}v_2)} \\ (Qx_1 + Px_3)\sqrt{(K_{n\_m}N_2 + K_{n\_s}N_1 + K_g g - K_{v\_m}v_2 + K_{v\_s}v_1)} \end{bmatrix} \tag{22}$$

and the structure of close loop system is shown in Fig. 3, where U_1 and U_2 are defined in (22).

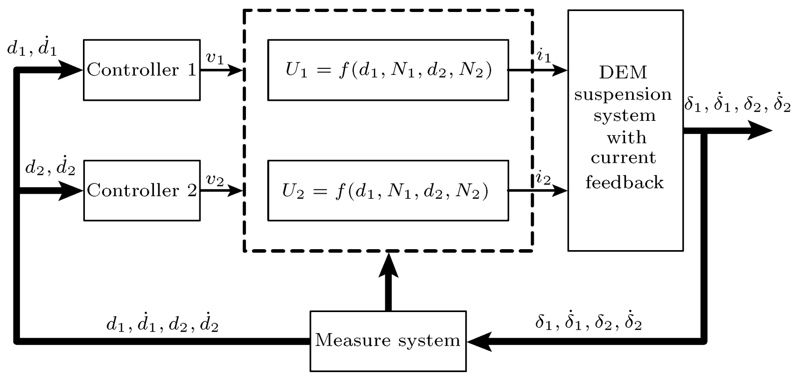

Fig. 3 The close loop system

4.2 System analysis

Substitution of (22) into (6) gives

$$\begin{cases} F_1 = K(K_{n\_m}N_1 + K_{n\_s}N_2 + K_g g - K_{v\_m}v_1 + K_{v\_s}v_2) \\ F_2 = K(K_{n\_m}N_2 + K_{n\_s}N_1 + K_g g - K_{v\_m}v_2 + K_{v\_s}v_1) \end{cases} \tag{23}$$

Then (3) can be rewritten as

$$\begin{cases} \ddot{d}_1 = v_1 \\ \ddot{d}_2 = v_2 \end{cases} \tag{24}$$

The result above is obtained under the assumption without disturbance. The load forces have been modeled in the mathematical model, so the relations between input and output do not include N_1 and N_2, that is to say, N_1 and N_2 will not affect the external characteristics of the close loop system. Let ΔN_1 and ΔN_2 denote the disturbance forces due to change of load or external disturbance which are unmodeled; then the relations from input to output are given by

$$\begin{aligned} \ddot{d}_1 &= C_K \times \Delta N_1 + D_K \times \Delta N_2 + v_1 \\ \ddot{d}_2 &= D_K \times \Delta N_1 + C_K \times \Delta N_2 + v_2 \end{aligned} \tag{25}$$

In order to reject the external disturbance force, we can take the following measures:

1) Measure the disturbance forces using force sensors and introduce them into the model.

2) Introduce integral tache into the controller to reject the change of load.

5 Simulation and experiment

5.1 Simulation and analysis

The simulation model is built in Simulink, and the physical parameters of the model are the same as the prototype shown in Table 1. δ_0 is the given gap value.

Table 1 Parameters used in simulation

S (m^2)	L (m)	l (m)	m (Kg)	I (Kg×m^2)	N	N_1 (N)	N_2 (N)	δ_0 (m)
0.0015	0.3	0.168	14.852	0.5648	663	36.5	36.5	0.005

To verify the performance of the proposed decoupling controller, we design a PID controller based on the single electromagnet as the referenced object (the referenced controller for short). The simulation results are shown in Fig. 4. The results of the referenced controller are shown in dashed line and the results of the decoupling controller is shown in real line.

1) The performance of load disturbance rejection. Assume that the DEM suspension system is in the steady state. At the 3rd second a load disturbance is exerted on point B. The gap response is shown in Fig. 4(a). It is obvious that the performance of load disturbance rejection of the decoupling controller is much better than that of the referenced controller. The decoupling controller takes the loads of the two points as dynamic parameters and takes them into account in the controller structure, so each point can not only reject the load disturbance of its own but also reject the coupling due to the load disturbance of the other point. In practice because of the delay of control and delay characteristic of the current loop, the gap values of the two points need an adjusting process to revert to the given gap value after load disturbance.

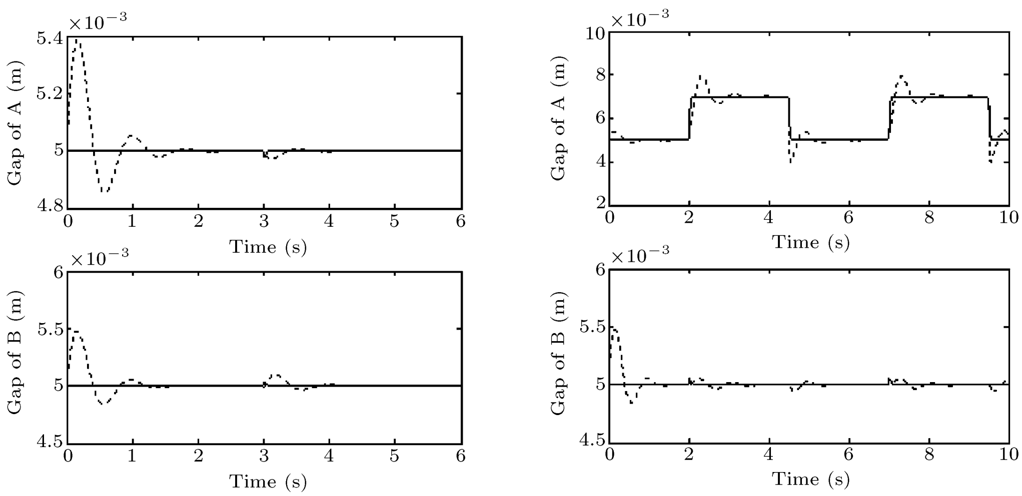

(a) Response to load disturbance (b) Response to gap disturbance

Fig. 4 Simulation results

2) Performance of gap disturbance rejection. Assume that the DEM suspension system is in the steady state. At the 2nd second, a square wave with period of 5s and amplitude of 0.002m is added to the gap value of point A. The gap response is shown in Fig. 4(b). It can be seen that the performance of gap disturbance rejection of the decoupling controller is much better than that of the referenced controller. In the ideal condition the state of one point will not be influenced when the state of the other point is disturbed if the DEM suspension system is controlled by the decoupling controller.

The simulation results show that the nonlinear decoupling control system can realize the electrical decoupling for the DEM suspension system.

5.2 Experiment and analysis

The controller is realized in a digital circuit based on ADSP21061. The experiment results are shown in Fig. 5. Curve 1 is the gap response of the system controlled by the decoupling controller and curve 2 is the gap response of the system controlled by the referenced controller. Fig. 5(a) is the response to load disturbance. When the DEM suspension system is in steady state, a poise is added to one point, and the gap response of the other point is shown. Fig. 5(b) is the response to gap disturbance. A square wave signal with a certain period and amplitude is added to the signal from the sensor of one point, and the gap of the other point is shown.

The experimental results are similar to the simulation results and it is shown that the performances of decoupling controller are much better then those of the referenced controller.

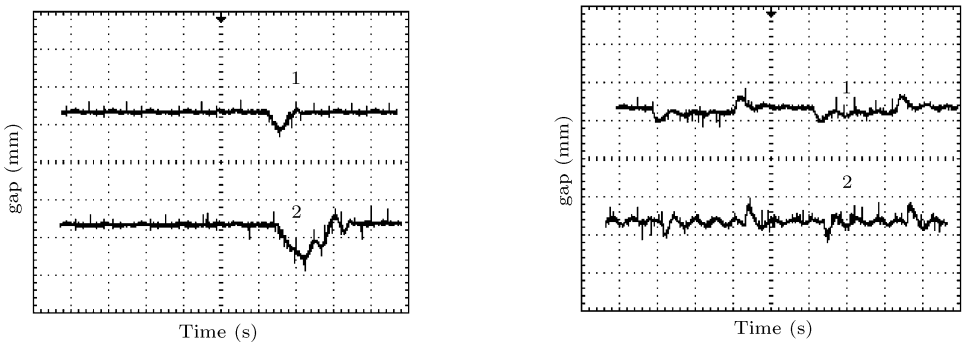

(a) Response to load disturbance coupling (b) Response to gap disturbance coupling

Fig. 5 Experiment results

6 Conclusions

In the present paper, we propose a nonlinear decoupling controller to solve the coupling problem between two groups of electromagnets inside of a module of the maglev train. The module is simplified as a DEM suspension system. The design procedure is carried out with feedback linearization and state feedback. The performances of load and gap disturbance rejection are tested in simulation and experiment. The results show that the proposed control method can solve the coupling problem efficiently.

References

1 Zhang K, Li J, Chang W S. Structure decoupling analysis of maglev train bogie. *Electric Drive for Locomotives*, 2005, **39**(1): 22∼23

2 Sinha P K, Pechev A N. Model reference adaptive control of a maglev system with stable maximum descent criterion. *Automatica*, 1999, **35**(8): 1457∼1465

3 Walter Barie, John Chiasson. Linear and nonlinear state-space controllers for magnetic levitation. *International Journal of Systems Science*, 1996, **27**(11): 1153∼1163

4 Toru Namerikawa, Masayuki Fujita. Uncertainty structure and μ-synthesis of a magnetic suspension system. *T. IEE Japan*, 2001, **121-C**(6): 1080∼1087

5 Liu D S, Li J, Zhang K. The design of the nonlinear suspension controller for ems maglev train based on feedback linearization. *Journal of National University of Defense Technology*, 2005, **27**(2): 96∼101

6 Liu D S, Li J, Chang W S. Internal model control for magnetic suspension system. In: IEEE Proceedings of the 4th International Conference on Machine Learning and Cybernetics, Guangzhou, China: IEEE Press, 2005. **1**: 482∼487

7 Li Y G, Chang W S. Cascade control of an ems maglev vehicle′s levitation control system. *Acta Automatica Sinica*, 1999, **25**(2): 247∼251

8 Zheng X J, Wu J J, Zhou Y H. Numerical analyses on dynamic control of five degree-of-freedom maglev vehicle moving on flexible guideways. *Journal of Sound and Vibration*, 2000, **235**(1): 43∼61

9 Hassan K Khalil. Nonlinear Systems, Second Edition, Michigan State University, 1996. 519∼569

LIU De-Sheng Received his bachelor degree from National University of Defense Technology in 2000. Now he is a Ph. D. candidate in Maglev Center at National University of Defense Technology. His research interest includes suspension control technology of maglev train.

LI Jie Received his bachelor and Ph. D. degrees from National University of Defense Technology in 1994 and 1999, respectively. From 1999 to 2001, he was post doctor in the Hong Kong University of Science and Technology. Now he is an associate professor at National University of Defense Technology and the director of Maglev Center. His research interest includes maglev system.

ZHANG Kun Received his bachelor and Ph. D. degrees from National University of Defense Technology in 1998 and 2004, respectively. Now he is a lecturer at National University of Defense Technology. His research interest includes suspension control technology of maglev train.